INTERNATIONAL JOURNAL FOR NUMERICAL METHODS IN ENGINEERING, VOL. 39, 1859–1878 (1996)

THE *p*-VERSION OF THE FINITE ELEMENT METHOD IN INCREMENTAL ELASTO-PLASTIC ANALYSIS

STEFAN M. HOLZER

Informationsverarbeitung im Konstruktiven Ingenieurbau, Universität Stuttgart, Pfaffenwaldring 7 D-70550 Germany

ZOHAR YOSIBASH

Pearlstone Center for Aeronautical Engineering Studies, Department of Mechanical Engineering, Ben Gurion University of the Negev, PO Box 653, Beer-Sheva 84 105, Israel

SUMMARY

Whereas the higher-order versions of the finite element method (*p*- and *hp*-versions) are fairly well established as highly efficient methods for monitoring and controlling the discretization error in linear problems, little has been done to exploit their benefits in elasto-plastic structural analysis. In this paper, we discuss which aspects of incremental elasto-plastic finite element analysis are particularly amenable to improvements by the *p*-version. These theoretical considerations are supported by several numerical experiments. First, we study an example for which an analytical solution is available. It is demonstrated that the *p*-version performs very well even in cycles of elasto-plastic loading and unloading, not only as compared with the traditional *h*-version but also with respect to the exact solution. Finally, an example of considerable practical importance—the analysis of a cold-working lug—is presented which demonstrates how the modelling tools offered by higher-order finite element techniques can contribute to an improved approximation of practical problems.

KEY WORDS: *p*-version; finite element method; elasto-plasticity; cold-working; non-linear problems; continuum mechanics

1. INTRODUCTION

Elasto-plastic analysis is of increasing importance in all fields of engineering sciences. However, real-life elasto-plastic problems are difficult to solve because they are non-linear in nature. Approximate numerical methods are required for solving practical problems of elasto-plasticity. The last two decades have witnessed a great deal of research for finding approximate solutions to elasto-plastic problems by the finite element method (FEM). References 1 provides an excellent review of the techniques of elasto-plastic modelling in the framework of the finite element method.

Almost all research work on elasto-plastic finite element analysis was based on the traditional *h*-version of the finite element method. The theoretical basis of the *h*-version is explained in Reference 2; see e.g. Reference 3 for details on the application of the *h*-version to elasto-plasticity. Whereas a lot of attention has been focused on realistic material models, the equally important issue of the accuracy of numerical modelling, including questions of discretization errors and convergence of the error in energy norm, remain largely unaddressed (see, however, References 4 and 5).

During the last decade, techniques for monitoring the discretization error in finite element approximations have been studied thoroughly, and new strategies for an efficient minimization of the error in energy norm have been developed. In the *p*-version of the FEM, the polynomial

CCC 0029–5981/96/111859–20

Received 28 June 1994
Revised 6 June 1995

degree of the finite element approximation is increased to improve the accuracy of the solution, rather than following the traditional approach of mesh refinement (*h*-version). The *hp*-version combines mesh refinement and increasing polynomial degrees.

The theoretical basis and convergence properties of the *h*-, *p*-, and *hp*-versions of the FEM for linear elliptic problems have been well established. Reference 6 provides a survey of the state-of-the-art of the *p*- and *hp*-versions of the finite element method based on the displacement formulation. By all measures of performance, the higher-order-methods provide superior accuracy (with respect to the discretization error) than their *h*-version counterpart for a large class of *linear* problems including linear elasticity.

The performance of the *p*-version for elasto-plastic stress analysis problems has not been investigated until very recently. To the authors' knowledge, the first numerical experiments which include *incremental elasto-plastic material models* in the frame of higher-order finite element methods have been reported in Reference 7. However, at that time no further discussion or evaluation of the efficiency of the *p*-version for this class of problems has been given. The first author of the present study has developed an experimental finite element code named FEASIBLE (cf. Reference 7) which includes *p*-version capabilities and provides elasto-plastic material laws as well as multi-stage analysis. This implementation has been employed for the numerical examples included in Sections 5 and 6.

Recently, the applicability of the *p*-version for solving elasto-plastic problems, using the *deformation theory of plasticity*, has been investigated numerically in Reference 8. This study shows that, even though the deformation theory is, strictly speaking, restricted to cases where the principal stresses remain proportional to each other throughout the plastic process, both theories yield very similar results in many cases. However, the problem categories amenable to the deformation theory do not include unloading and cyclic elasto-plastic processes.

Therefore, the present paper focuses on the *incremental theory of plasticity* (for an introduction, see e.g. References 1 and 9). The paper is organized as follows: We identify those subtasks of the elasto-plastic finite element procedure which determine the computational performance and accuracy of the numerical analysis. Subsequently, we discuss in which steps of the elasto-plastic analysis we would expect improvements when switching to the *p*-version. It is shown that many of the advantages of the *p*-version in purely linear analysis carry over to elasto-plastic problems. A numerical study of the loading and unloading of a thick-walled cylinder under internal pressure is presented. For this problem, an exact solution is available. The analytical results are then compared with the finite element solutions obtained by the *p*-version and the *h*-version. We demonstrate that the *p*-version method performs very well, also as compared with the *h*-version.

Finally, some unique features of the *p*-version finite element code are illustrated which permit realistic modelling of practical engineering problems. The finite element solution to a lug which undergoes cold-work expansion is provided and compared with the approximate closed-form solution often used in practice by engineers. This example demonstrates that many cold-working problems demand a finite element analysis when other than very crude accuracy requirements are imposed. Furthermore, it shows that the *p*-version of the FEM makes the analysis of such problems very convenient and easy as well as reliable and robust.

2. FINITE ELEMENT APPROXIMATION

Once a specific material model has been selected and the geometrical and mechanical idealization of the structure has been determined, the problem of structural analysis is cast in the form of a purely mathematical problem. The finite element method is a tool for solving this well-defined mathematical problem approximately. The primary aim of the finite element analysis is to find as

good an approximation to the exact solution of the mathematical problem as can be obtained with a given amount of engineering work and computer resources. The issue of how well the selected mathematical model corresponds to the physical reality is to be treated completely independently of the issue of the numerical accuracy of the finite element solution. In the present paper, we focus exclusively on the errors introduced by the finite element discretization, not on the physical modelling issue.

The finite element method based on the displacement formulation starts by minimizing the functional of the potential energy

$$\Pi(\mathbf{u}) = \tfrac{1}{2}B(\mathbf{u}, \mathbf{u}) - F(\mathbf{u}) \tag{1}$$

over a finite dimensional subset $\tilde{S}$ of the space $\tilde{E}(\Omega)$ of functions which have finite strain energy over the domain Ω and fulfil the displacement boundary conditions. Here, the bilinear form $\frac{1}{2}B(\mathbf{u}, \mathbf{u})$ denotes the strain energy corresponding to some displacement field $\mathbf{u}$ and $F(\mathbf{u})$ the work of the applied loads. Thus, an approximation $u_{FE} \in \tilde{S}(\Omega)$, minimizing $\Pi(\mathbf{u})$ over $\tilde{S}(\Omega)$, is obtained, whereas the exact solution $\mathbf{u}_{ex}$ minimizes $\Pi(\mathbf{u})$ over $\tilde{E}(\Omega)$.

Consequently, for an assessment of the efficiency of a specific finite element scheme, the magnitude of the discretization error in the energy norm is monitored as a function of the number of degrees of freedom N used in the finite element approximation $\mathbf{u}_{FE}$. The error in energy norm is defined by

$$\| e \|_E \stackrel{\text{def}}{=} \sqrt{\Pi(\mathbf{u}_{ex} - \mathbf{u}_{FE})} \tag{2}$$

In the present study, the p-version of the FEM is applied in the form of a uniform p-extension, increasing the polynomial degree of the approximation uniformly on the entire mesh. As far as linear analysis is concerned, the p-version is distinctly superior to the h-version for problems which have an exact solution that is analytic throughout the domain. In such cases, exponential convergence (i.e. $\| e \|_E = ce^{-\beta\sqrt{N}}$) can be achieved asymptotically ($N \to \infty$) with simple finite element meshes, whereas the convergence of the h-version is only algebraic (i.e. $\| e \|_E = cN^{-\beta}$). The actual value of the convergence rate β depends on the precise character of the exact solution.

Even for problems which include a finite number of points where singularities occur in the stresses, the p-version converges (algebraically) at least twice as fast as the h-version (i.e. a better value of β can be obtained by the p-version than by the h-version), even on meshes without any local refinement. Resorting to the hp-extension, i.e. performing simultaneous mesh refinement and increase of polynomial degree, the exponential convergence in energy norm can be recovered even for these singular problems. However, for such problems, convergence characteristics which are significantly better than algebraic can also be obtained in the pre-asymptotic range (i.e. for practical N) by performing the p-extension on a geometrically graded mesh, cf. Reference 6. The appropriate mesh refinement is done in advance then, determining the refinement areas by *a priori* criteria, rather than refining the mesh simultaneously with the p-extension.

In elasto-plastic analysis, $\Pi(\mathbf{u})$ is a non-linear function of $\mathbf{u}$ so that the properties of the FEM for linear analysis do not carry over to elasto-plasticity directly. However, in the incremental theory of plasticity, we solve a sequence of linearized problems with the same geometry, but strain-dependent material properties and loads. The final solution is obtained as the sum of those of the quasi-linear steps. Therefore, the overall performance of the non-linear analysis will be determined by the smoothness of the exact solutions of the stepwise problems.

The smoothness properties of the exact solution of purely elastic problems are well known and can generally be determined *a priori* from the geometric shape and the boundary conditions; on the other hand, little has been done yet to inquire how much the introduction of elasto-plastic

material behaviour changes the smoothness properties of the corresponding purely elastic solution.

However, when deciding which finite element method is more appropriate when solving an elasto-plastic problem, the question of smoothness is of little relevance because the higher-order methods perform significantly better for problems in *any of the two categories of smoothness* discussed above. This important fact is often overlooked.

Furthermore, it is worth noting that the elastic-plastic material is still characterized by continuous strains so that elasto-plasticity does *not introduce* any kind of an abrupt '*material interface*' inside the elements. Such a situation might cause the *p*-version to yield oscillatory answers. However, it does not occur in small-strain elasto-plasticity since there is always a continuous change in the material properties, even though the one-dimensional ideal elasto-plastic stress–strain relationship intuitively suggests some kind of 'discontinuity'. Even upon unloading and reloading, the strains and consequently the material properties (directly depending on the strains) remain continuous.

All *contained plastic flow problems* fall into the category of completely continuous strains and, consequently, the corresponding displacements can be expected to be at least not much more unsmooth than those resulting from purely elastic problems.

As far as *uncontained plastic flow* is concerned, the underlying mathematical problem changes from the elliptic to the hyperbolic type, including possible bifurcations, multiplicity of the solution, and the like; such problems are strictly *beyond the limits* of small-strain elasto-plastic analysis for both the *h*- and *p*-versions of the FEM. They cannot be solved by methods based on the principle of minimum potential energy. Of course, the physical problem finally emerges into unrestricted plastic flow. However, the FEM does not directly model the physical problem, but is only a tool for solving a mathematical problem. If unrestricted plastic flow is to be analysed, a different mathematical model has to be used, *not just a different type of finite element approximation.*

The accuracy of the strains computed from the finite element solution is even more important in elasto-plastic analysis than in purely linear problems because the stress–strain law itself depends on the strains. We can expect accurate results only if the input to the constitutive law is sufficiently accurate. Furthermore, errors tend to accumulate in a prolonged incremental computation with many load steps.

A recent study[10] investigates numerically the pointwise quality of strains computed directly from the finite element approximation of the displacement field for linear problems. This is exactly the technique that will be employed in an elasto-plastic computation to determine the current material properties. The numerical investigation[10] identifies various patterns of convergence and shows that in all cases and for a wide variety of stress concentration factors (a smoothness criterion) the *p*-version outperforms the *h*-version. Furthermore, it is evident that very small errors in the energy norm are usually required to achieve sufficient accuracy of the pointwise strains, even for quite smooth solutions. Such global accuracy levels are impractical for an *h*-version approach due to the slow convergence of this method.

In summary, all considerations indicate that the *p*-version of the FEM will be beneficial for elasto-plastic computations, and there is no indication that the *p*-version might give rise to any new numerical problems not encountered in the *h*-version. Our numerical examples strongly support this.

3. NUMERICAL ASPECTS OF J_2 PLASTICITY

In the present paper, we are dealing with the application of the *p*-version of the FEM to problems from metal plasticity. The computations are based on the ideal elastic-plastic J_2 flow theory, using

the von Mises yield law. Further assumptions include small displacements and small strains. The incremental formulation of the von Mises yield law starts with the following assumptions:

The total strain increment can be decomposed into a purely elastic and a purely plastic part:

$$d\varepsilon = d\varepsilon_{el} + d\varepsilon_{pl} \tag{3}$$

We assume the engineering definition of the strain vector.

The yield criterion is independent of the hydrostatic pressure and of the third invariant of the deviatoric stress tensor:

$$F = 3J_2 - \sigma_y^2 \tag{4}$$

J_2 denotes the second invariant of the deviatoric stress tensor and σ_y the uniaxial yield stress of the material. No strain hardening is assumed. Only stress states such that $F \leqslant 0$ are permissible. Once the stress path reaches $F = 0$ in a point, plastic strains will develop in that point upon further loading.

During a plastic loading increment, the stress state is confined to the yield surface given by equation (4):

$$dF = [\partial F/\partial\sigma]^t \, d\sigma = 0 \tag{5}$$

In equation (5), $d\sigma$ denotes the stress increment vector and the superscript t indicates transpose.

The direction of the plastic flow is given by (normality rule)

$$d\varepsilon_{pl} = d\lambda[\partial F/\partial\sigma] \tag{6}$$

Here, $d\lambda$ is a proportionality factor and σ denotes the stresses in vectorial notation. Using Hooke's law for the elastic part of the strains,

$$d\varepsilon_{el} = D^{-1} \, d\sigma \tag{7}$$

where D is the linear-elastic material matrix, formulas (3), (5) and (6) can be combined to determine the elasto-plastic stress increment

$$d\sigma = D_{ep} \, d\varepsilon = \left[D - \frac{D\left[\frac{\partial F}{\partial\sigma}\right]\left[\frac{\partial F}{\partial\sigma}\right]^t D}{\left[\frac{\partial F}{\partial\sigma}\right]^t D \left[\frac{\partial F}{\partial\sigma}\right]} \right] d\varepsilon \tag{8}$$

corresponding to a total strain increment $d\varepsilon$. Formula (8) defines the elasto-plastic material matrix D_{ep}. This relationship is needed in a finite element program to determine the tangential stiffness matrix for a Newton–Raphson method or a similar scheme. Furthermore, it can be used to integrate the constitutive law on the integration point level of the finite element method in case an explicit algorithm is to be used for that. Whereas the correctness of the tangent stiffness matrix has only an influence on the efficiency of the non-linear solver, the integration of the constitutive law has a direct impact on the accuracy of the final results.

Much attention has been dedicated to the accurate integration of the constitutive law during the last two decades (cf. References 11–14). A comprehensive scheme of error control and quality assurance in the FEM has to include this aspect, which is, however, independent of the finite element discretization technique. With a view to practical applications, and especially with

respect to the complicated plastic laws which become increasingly common in rock mechanics and concrete modelling, the authors of the present study favour a fully general implicit scheme similar to the one presented in Reference 14. However, at present, only the traditional tangent-radial return method has been implemented. This simple scheme can be considered sufficiently accurate for the von Mises yield criterion without hardening provided that small steps are used for the integration of the constitutive law.

However, the most challenging computational issue specifically related to the use of J_2 flow rules is created by the condition that the plastic strains correspond to an incompressible mode of deformation (note that it follows from equations (4) and (6) that the plastic strain increments have no volumetric component): Starting from a compressible elastic behaviour, the material becomes progressively more incompressible during the elasto-plastic deformation process as the amount of plastic strain increases as compared to the elastic strain. This will eventually lead to a severe locking problem in the traditional h-version of the finite element method if the displacement formulation is used. The problem of incompressibility locking in J_2 plasticity has already been studied in Reference 15, and various schemes have been devised to avoid the locking, either by 'reduced integration' or by introducing an independent approximation of the hydrostatic pressure. Today, most approaches use the mixed finite element method resulting from the latter idea, entailing all the disadvantages and additional complications inherent to mixed methods.

On the other hand, the problem of locking due to incompressibility has been studied extensively for the p-version of the finite element method (see References 16–18), and it has been shown that no locking effects occur when the polynomial degree p is greater than four. No special precautions or mixed methods have to be introduced to obtain accurate results.

Our numerical experiments will demonstrate clearly that locking due to incompressibility does not occur in the p-version analysis of the elastoplastic problem.

4. IMPLEMENTATION

In many details, the implementation of an elasto-plastic material law in a p-version FEM code is identical to a standard h-version implementation. Therefore, we summarize only briefly the main features of the implementation used for the present study.

First, we carry out a purely linear elastic analysis and perform a uniform p-extension, starting at $p=1$ (piecewise linear approximation). The maximum polynomial degree available is $p=8$. The convergence of the strain energy is monitored. Based on the assumption that the error in energy norm converges algebraically, a very reliable estimate of the exact energy can be obtained by extrapolation from three different p-levels (cf. Reference 6). Throughout the present study, the space of hierarchical tensor product trial functions has been used (product space).

To avoid errors in the linear solution by approximate geometrical mapping, we always use the blending-function method (see Reference 6) to describe curved boundaries accurately. Therefore, we can use very large elements even in the presence of curved boundaries.

When the error estimate for the purely linear solution reaches a user-defined threshold, the non-linear computation starts. There is no guarantee that the non-linear solution will be of the same order of accuracy as the linear solution, but we rather expect the non-linear solution to be less accurate. We have already seen that e.g. incompressibility effects which are not originally present in the system will be introduced by the plastic material law, and those effects will slow down the convergence of the error in energy norm. Therefore, it seems reasonable to impose very restrictive accuracy requirements on the linear solution. In our practical computations, as a rule of thumb, we set the desired accuracy of the linear solution to about 10 per cent of what we would consider reasonable for a purely elastic analysis.

The next step is to determine at which fraction of the total imposed load the system will start to yield. The remaining load is divided into a number of load increments, and in each of these the Newton–Raphson method with a consistent tangent predictor is applied. The Newton–Raphson iterations are stopped when both the relative magnitude of residual force vector and of the change in the incremental displacements in either the Euclidean or the maximum norm are smaller than a prescribed threshold. In each load increment, a check for elastic unloading is performed in every integration point.

Finally, stress results are available only in the integration points since the incremental elasto-plastic law has been evaluated only there. To obtain stress results, elsewhere a least-squares approximation for each of the components of the stress vector is computed for each element individually. For this least-squares fit, we employ the trial functions corresponding to the polynomial level used in the finite element approximation of the displacements. The issue of interpolating the stress results has not been fully investigated in the present study. It might be preferable not to approximate each stress component individually, but separate the hydrostatic part first, and do the least-squares fit afterwards on the hydrostatic and deviatoric parts individually. The effects of the stress evaluation procedure on the final pointwise stress accuracy yet need to be investigated in more detail. The current procedure is only a pragmatic approach to the problem.

5. THE THICK-WALLED TUBE UNDER INTERNAL PRESSURE

First, we study an-example for which an analytical solution is available, the thick-walled tube under internal pressure. The analytical solution for both the loading and the unloading—including elasto-plastic re-loading in the reverse direction—has been given in Reference 19. It is one of the few elasto-plastic two-dimensional problems for which an analytical solution even for the unloading is available, and therefore we use it as a basis for the evaluation of the numerical quality of the h- and p-versions of the finite element method.

However, this problem is also of considerable practical interest since the pressurized tube may be used as a model for the cold-working of holes e.g. in aircraft engineering. Rich *et al.*[20] suggest to use the analytical solution for the analysis of a wide range of cold-worked holes, and in our practical application example, we will study how well this solution is suited for a cold-worked lug.

Cold-working is a process which is used to produce favourable stresses that significantly reduce the effects of stress concentration around a hole. In this method, an oversized and tapered mandrel, sometimes with a lubricated sleeve, is pulled through the hole to be cold-worked. Upon the removal of the mandrel, the hole is surrounded by a region of residual compressive stresses. This method is generally used for holes at the time of aircraft manufacture, as well as during service, to increase the fatigue life to structural components.

5.1. Analytical solution

The analytical solution for the problem of the tube under internal pressure has been given in Reference 19 and applied to the cold-working process in Reference 20. The following assumptions are adopted in the analysis:

(1) elastic-perfectly plastic material model,
(2) plane strain situation,
(3) von Mises yield condition,
(4) incompressibility of both the elastic and plastic zones (no analytical exact solution exists deformation).

In the application to cold-working, the mandrel is assumed to remain purely elastic. Under these assumptions, the solution can be obtained in closed form, which is very well suited for comparison with numerical approximations. Dropping the incompressibility assumption, a closed-form solution is no longer available.

Notation. Consider a tube with an internal radius a and an external radius b, Young's modulus E_p, Poisson ratio ν_p and uni-axial yield stress σ_y. Denote the modulus of elasticity for the mandrel by E_b, its Poisson ratio by ν_b and its radius by $a + I$. The difference I between the radii of the mandrel and the hole is called interference.

Upon inserting the mandrel into the tube, a plastic zone of radius ρ is created. This radius is defined by the following implicit equation (if no solution exists for the equation, the interference is simply too small to create a plastic zone):

$$I/a - \frac{\sigma_y}{\sqrt{3}E_b}\left[0{\cdot}52\left(2\ln\frac{\rho}{a}+1-\frac{\rho^2}{b^2}\right)+1{\cdot}5\frac{\rho^2}{a^2}\frac{E_b}{E_p}\right]=0 \tag{9}$$

and the pressure between the mandrel and the hole can be shown to be

$$P=\frac{\sigma_y}{\sqrt{3}}\left[2\ln\frac{\rho}{a}+1-\frac{\rho^2}{b^2}\right] \tag{10}$$

If $P \geqslant 2(\sigma_y/\sqrt{3})\ln(b/a)$, then the entire cylinder becomes plastic, and this case is of no interest for us.

The circumferential stresses around the hole are given by

$$\sigma_\theta=\begin{cases}\dfrac{\sigma_y}{\sqrt{3}}\left[2\ln\dfrac{r}{\rho}+1+\dfrac{\rho^2}{b^2}\right] & a\leqslant r\leqslant\rho\\[2ex] \dfrac{\sigma_y}{\sqrt{3}}\left[\dfrac{\rho^2}{b^2}+\dfrac{\rho^2}{r^2}\right] & \rho\leqslant r\leqslant b\end{cases} \tag{11}$$

Upon removal of the mandrel, the tube undergoes an elastic unloading. If $P > 2(\sigma_y/\sqrt{3})(1-a^2/b^2)$, no reverse yielding occurs, and the residual circumferential stresses are given by

$$\sigma_\theta=\begin{cases}\dfrac{\sigma_y}{\sqrt{3}}\left\{\left[2\ln\dfrac{r}{\rho}+1+\dfrac{\rho^2}{b^2}\right]-\left[2\ln\dfrac{\rho}{a}+1-\dfrac{\rho^2}{b^2}\right]\dfrac{a^2(r^2+b^2)}{r^2(b^2-a^2)}\right\} & a\leqslant r\leqslant\rho\\[2ex] \dfrac{\sigma_y}{\sqrt{3}}\left\{\left[\dfrac{\rho^2}{b^2}+\dfrac{\rho^2}{r^2}\right]-\left[2\ln\dfrac{\rho}{a}+1-\dfrac{\rho^2}{b^2}\right]\dfrac{a^2(r^2+b^2)}{r^2(b^2-a^2)}\right\} & \rho\leqslant r\leqslant b\end{cases} \tag{12}$$

Otherwise, compressive yielding occurs in the zone $a \leqslant r \leqslant \rho_R$, where ρ_R is given by the implicit equation:

$$2\ln\frac{a}{\rho_R}-1+\frac{\rho_R^2}{b^2}+\frac{P\sqrt{3}}{2\sigma_y}=0 \tag{13}$$

In this case, the circumferential stress is

$$\sigma_\theta = \begin{cases} \dfrac{\sigma_y}{\sqrt{3}}\left\{\left[2\ln\dfrac{r}{\rho}+1+\dfrac{\rho^2}{b^2}\right]-2\left[2\ln\dfrac{r}{\rho_R}+1+\dfrac{\rho_R^2}{b^2}\right]\right\} & a \leqslant r \leqslant \rho_R \\ \dfrac{\sigma_y}{\sqrt{3}}\left\{\left[2\ln\dfrac{r}{\rho}+1+\dfrac{\rho^2}{b^2}\right]-2\left[\dfrac{\rho_R^2}{b^2}+\dfrac{\rho_R^2}{r^2}\right]\right\} & \rho_R \leqslant r \leqslant \rho \\ \dfrac{\sigma_y}{\sqrt{3}}\left\{\left[\dfrac{\rho^2}{b^2}+\dfrac{\rho^2}{r^2}\right]-2\left[\dfrac{\rho_R^2}{b^2}+\dfrac{\rho_R^2}{r^2}\right]\right\} & \rho \leqslant r \leqslant b \end{cases} \tag{14}$$

This problem is suitable for both the incremental and deformation theories of plasticity because it is axisymmetric and the stresses are proportional.

Note that equation (6) in Reference 20 is not correct which renders the stresses in the compressive plastic zone around the hole after unloading. The correct solution is found in Reference 19.

5.2. *Numerical examples*

The problem described in the previous section is solved by the p-version as well as the h-version of the FEM. The finite element solutions to this problem will demonstrate the capabilities of the p-version and its accuracy.

Comparison with the exact solution. We study a tube with an internal radius $a = 1{\cdot}5$ in and an outer radius $b = 4{\cdot}0$ in subjected to a cold-working process. A plane strain situation is assumed. A pressure $P = 62\,000$ psi is applied to both the inner side of the tube and the outer face of the mandrel. We determine the corresponding interference level as the sum of the radial displacements of both bodies. Thus, an interference $I = 0{\cdot}03399$ in is obtained. The material properties of the tube are defined by $E_p = 10\,000\,000$ psi, the uniaxial yield stress $\sigma_y = 58\,000$ psi, and $\nu_p = 0{\cdot}49$. We select this value of the Poisson ratio in order to be close to the exact analytical solution which assumes elastically incompressible material. The displacement-based finite element schemes cannot be applied if $\nu = 0{\cdot}5$ exactly. The mandrel's material properties are taken to be $E_b = 30\,000\,000$ psi, and $\nu_b = 0{\cdot}3$. All finite element computations are based on an elastic-perfectly plastic von Mises yield law.

Exploiting symmetry, only one quarter of the domain was analysed. The radial displacements are constant along the perimeter. For each of the two versions of the FEM, two different meshes have been analysed. The purely elastic mandrel has been studied only in one simple p-version mesh, imposing extremely high accuracy requirements.

In Figure 1, the meshes used for the cylinder in the p-version are shown. We use a uniform mesh of two elements and a graded mesh of six elements for the representation of the tube. The boundary conditions are $u_y = 0$ on edge A–B, $u_x = 0$ on edge C–D, and $t_n = -P$ on A–D, where t_n denotes the normal traction. The other boundary conditions are traction-free. The p-level is increased on each element until the estimated global error in energy norm is decreasing below 0·1 per cent. We use the product space and the p level is uniform throughout the mesh. On the coarse mesh, the error estimate indicates that the desired accuracy threshold has been reached when we use $p = 8$, whereas $p = 5$ is sufficient for reducing the error estimate below the threshold on the finer mesh.

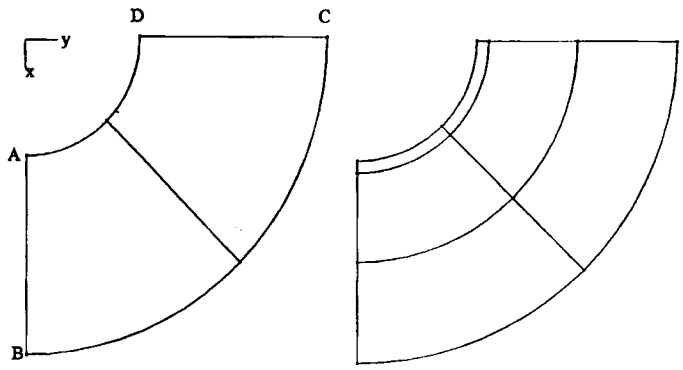

Figure 1. Meshes used in the p-version analysis of the tube under internal pressure

For the h-version, we use meshes consisting of 70 eight-noded elements and 140 eight-noded elements, respectively. Both meshes are graded in the radial direction such that the biggest element is ten times bigger than the smallest. A mesh consisting of 300 eight-noded elements was also analysed to make sure that the mesh of 140 elements was fine enough in the circumferential direction. The three different h-version meshes are shown in Figure 2. The results obtained with the 300-element mesh are practically identical to those of the 140-element mesh, so only the latter mesh is used in our examples.

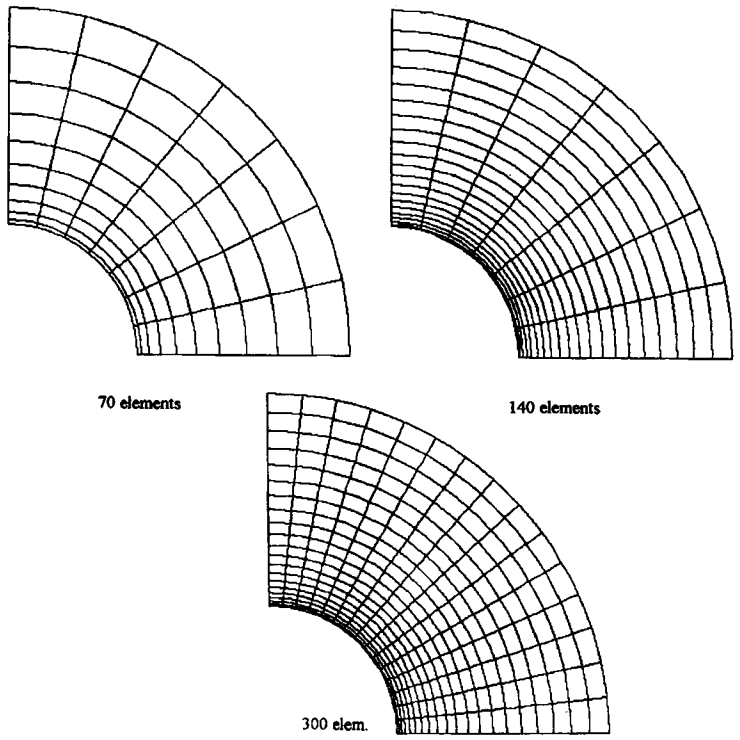

Figure 2. Meshes used in the h-version analysis of the tube under internal pressure

Furthermore, we also analysed the mesh with 70 elements, employing nine-noded elements instead of the eight-noded elements. The trial function space associated with the nine-noded elements corresponds to the product space at $p=2$ in the p-version.

The h-version computations were carried out with the commercial finite element solver[21] ADINA. The ADINA system offers a special pressure-displacement element for incompressible materials, based on the mixed finite element formulation.[22] This element was used in the analysis.

For avoiding any influence of the size of the load increments and the accuracy of the equilibrium iterations in the non-linear computation, the load steps and equilibrium threshold have been varied in a very broad range and chosen such that the resulting solutions proved virtually independent of these parameters. At least 10 load steps have been used after reaching the elastic limit, and also for the elasto-plastic unloading, or rather, reverse loading. A large number of load steps was suggested by the fact that only the tangent-radial return method for integrating the constitutive law has been implemented in the research code until now. The effects of the accuracy bounds imposed on the loading/unloading procedure will not be considered in the following, as they turned out to be completely negligible in comparison to the differences in the results caused by the choice of the method for the finite element approximation.

In Figure 3, the exact analytical solution of the circumferential stress (σ_θ) for the loading case is compared with the p-version solution. The h-version solution with eight-noded elements and the exact solution are displayed in Figure 4. Note the very good agreement between the exact and the finite element solutions in the whole range, except at the interface between the elastic and plastic zones. At this location, the h-version solutions with the eight-noded elements tend to oscillate, and the quality of the results is questionable, whereas the p-version solution is much smoother and follows the exact solution more closely. The p-version merely produces smoothed stress results close to the elastic-plastic interface. It is clearly visible that the elasto-plastic radius (ρ) can easily be determined from the p-version solutions, but not so well from the solutions obtained by the h-version with eight-noded elements.

However, the h-version solution improves considerably when we employ the nine-noded elements instead. These elements have an additional 'internal mode' trial function. The corresponding results are displayed in Figure 5. No oscillations are present any more, even in the coarser mesh. The computer time for this analysis is somewhat greater than for the eight-noded

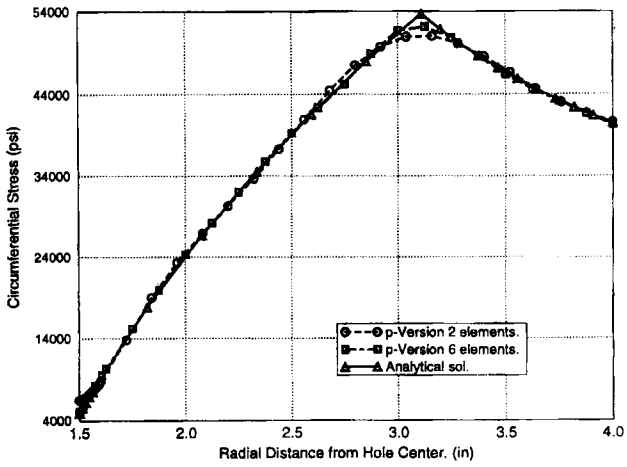

Figure 3. Circumferential stress in pressurized tube, loading case. Results of p-version FEM analysis an exact solution

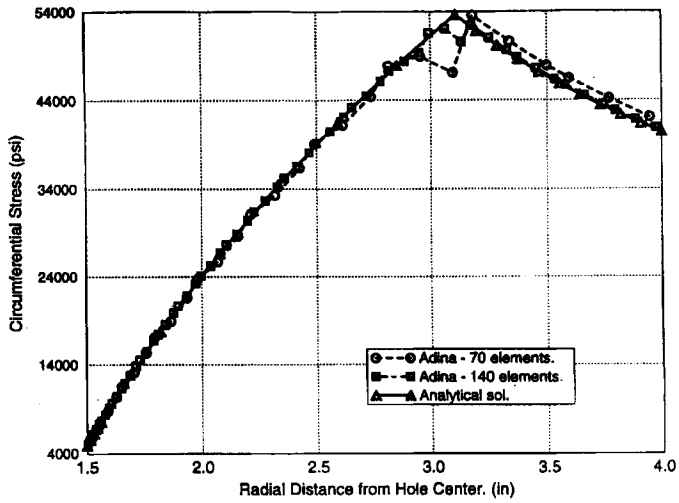

Figure 4. Circumferential stress in pressurized tube, loading case. Results of *h*-version FEM analysis with 8-noded elements and exact solution

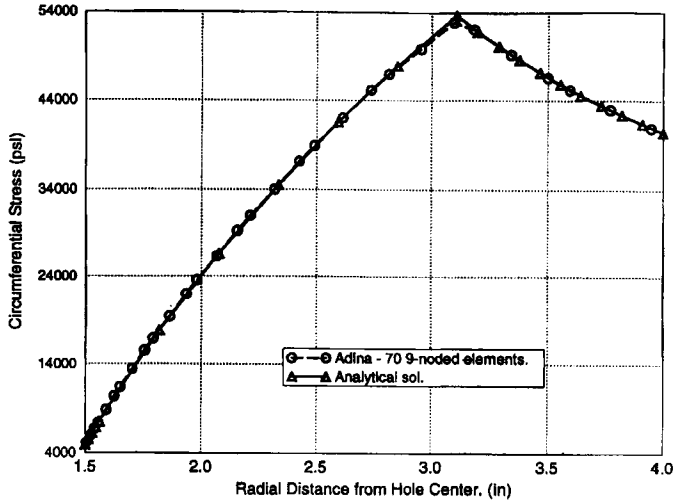

Figure 5. Circumferential stress in pressurized tube, loading case. Results of *h*-version FEM analysis with 9-noded elements

elements. It is interesting that, even in the *h*-version, obviously some degree of '*p*-extension' and switching to a different space of trial functions is required to capture the solution of this problem properly.

Upon removing the internal pressure, the tube first undergoes an elastic unloading; in the last stage of the unloading, reverse yielding occurs in the vicinity of the inner surface of the tube. The overall performance of the *h*-version as well as the *p*-version, compared to the exact analytic solution, is presented in Figures 6 and 7, respectively.

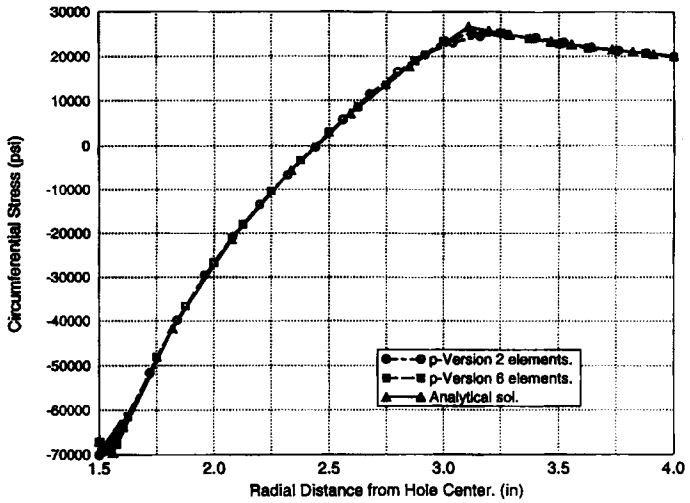

Figure 6. Circumferential stress in pressurized tube. Residual stress after cold-working. Results of p-version FEM analysis and exact solution

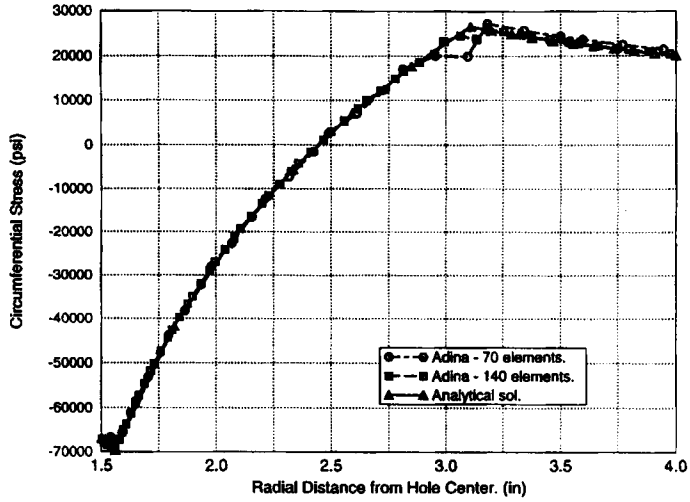

Figure 7. Circumferential stress in pressurized tube. Residual stress after cold-working. Results of h-version FEM analysis and exact solution

In Figures 8–10, we present 'zoomed' plots of the circumferential stresses in the reverse yielding zone. The same phenomenon as in the loading case is observed at the new elasto-plastic interface radius ρ_R: Both h-version meshes with eight-noded elements exhibit oscillations of the stress in the reverse yielding zone. Furthermore, it turns out that the 2-element p-version mesh is obviously unable to capture the very narrow zone of reverse yielding properly. Clearly, just one element in the radial direction is not sufficient. However, a very good solution is obtained with the six-element mesh and the p-version. Also, the solution of the h-version with nine-noded elements is quite accurate.

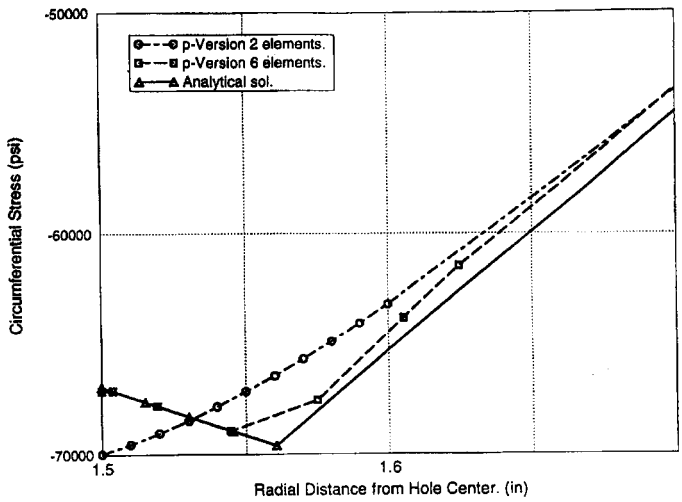

Figure 8. Circumferential stress in pressurized tube. Residual stress after cold-working. Results of *p*-version FEM analysis and exact solution. Zoom of zone of compressive plastification

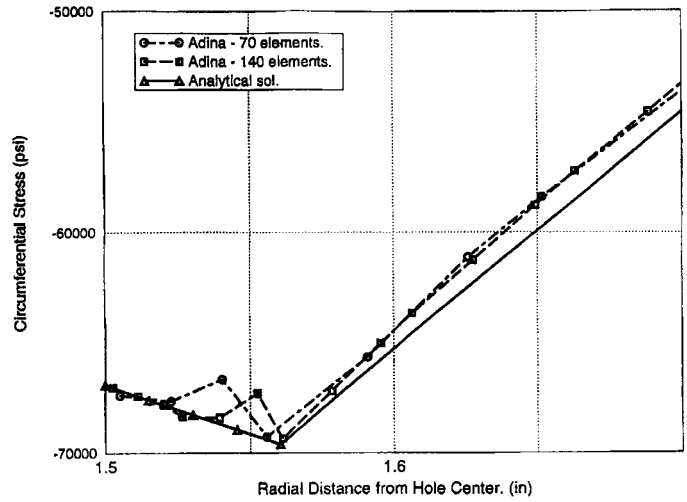

Figure 9. Circumferential stress in pressurized tube. Residual stress after cold-working. Results of *h*-version FEM analysis with 8-noded elements and exact solution. Zoom of zone of compressive plastification

In order to verify the smoothness of the material properties in this elasto-plastic computation, the condition number (ratio of the largest and smallest eigenvalue) of the tangential material matrix (stress–strain matrix) has been checked in all integration points during the loading and unloading process. The condition number changes very little during the loading and unloading and depends predominantly on the elastic material properties. This indicates that the influence of elasto-plasticity on the *smoothness* of the stress–strain law is very small.

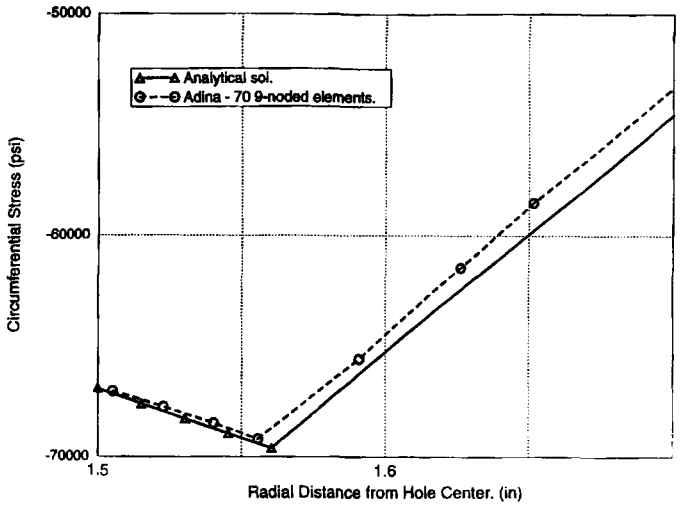

Figure 10. Circumferential stress in pressurized tube. Residual stress after cold-working. Results of h-version FEM analysis with 9-noded elements and exact solution. Zoom of zone of compressive plastification

Table I. Computation times and number of unknowns for the elasto-plastic loading and unloading of a tube under internal pressure ($\nu = 0{\cdot}49$)

	ADINA	FEASIBLE
Coarse mesh	82 s	88 s*
	450 d.o.f.	288 d.o.f.
Fine mesh	162 s	90 s†
	870 d.o.f.	456. d.o.f.

Note: The FEA solutions were computed on a Silicon Graphics SGI IRIS Indigo workstation (R3000, SPEC mark =26). The computation times reported do not include post-processing operations. The number of degrees of freedom does not include constrained degrees of freedom.
* Maximum p-level is 8, product space.
† Maximum p-level is 5, product space.

A rough comparison between the computation times of the finite element solutions (measured on an IRIS SGI workstation) is given in Table I. The computation times for the p-version include multiple purely elastic runs with increasing p-levels to minimize the error of the elastic solution. Table I demonstrates that the computer time resources required by the p-version and the h-version solutions are of roughly the same order of magnitude.

The realistic case of $\nu_p = 0{\cdot}3$ in the elastic zone. Usually, the Poisson ratio of engineering materials in the elastic region is close to 0·3. In the following, we use the finite element solution to show that the analytical solution based on the incompressibility assumption in the elastic region may be considered as a good approximation for the solution with $\nu_p = 0{\cdot}3$.

For this case, we select a smaller interference than before, $I = 0{\cdot}02$ in. This will emphasize the influence of the compressibility in the *elastic* zone since the extent of the plastic zone will be

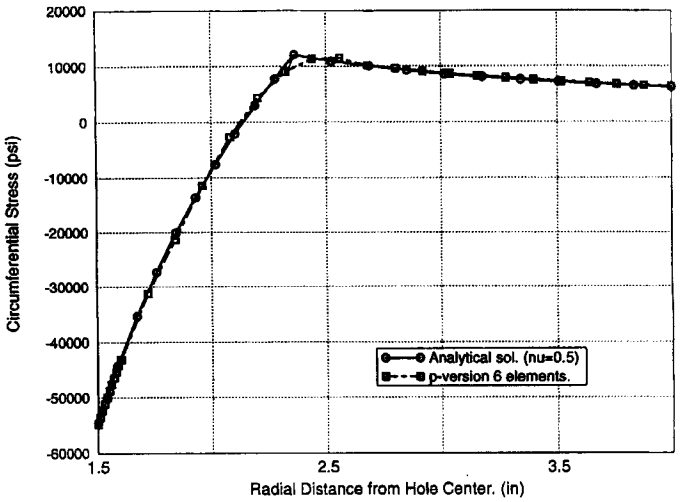

Figure 11. Circumferential stress in pressurized tube, $\nu = 0{\cdot}3$. Residual stress after cold-working. Results of p-version FEM analysis and analytical solution for $\nu = 0{\cdot}5$

smaller than before. Employing the six-element mesh with the p-version, and the 140-element mesh with the h-version, the corresponding pressure was calculated to be $P = 52\,200$ psi. The finite element solutions for $\nu_p = 0{\cdot}3$ are compared to the analytic solution (assuming $\nu_p = 0{\cdot}5$) in Figure 11. It is evident that the unrealistic assumption of incompressibility in the elastic region does not significantly affect the validity of the analytical solution for the practical case. The elasto-plastic radius, however, is smaller than the one predicted by the FEM solutions.

6. PRACTICAL APPLICATION: THE COLD-WORKING OF AN ATTACHMENT LUG

Usually, as a first approximation, engineers use the closed-form solution for a cold-worked cylinder given in Reference 20 in real-life problems, even though the geometry of the realistic problem is different from the cylinder. A cold-worked fastener hole located near a plate edge, or a lug, is usually idealized as a cold-worked tube having an inner radius equal to the hole radius, and an outer radius equal to the distance of the fastener hole from the edge. We show in the following that this approximation has considerable deficiencies and should be used only for fairly crude accuracy requirements.

In the case of the lug, which is no longer axisymmetric, the question of adequate finite modelling arises. The plastic zone is no longer bounded by a circle, and also the deformations of both the mandrel and the hole deviate from the purely circular shape. Therefore, a finite element analysis imposing uniform pressure or constant radial displacements on the hole does not reflect the true situation properly. Neither the final shape of the deformed mandrel and hole nor the pressure distribution is known *a priori*. Furthermore, even for the axisymmetric case of the tube (with corresponding dimensions), an analysis carried out with prescribed displacements equal to the interference (i.e. assuming a rigid mandrel) reveals considerable differences in the residual stresses (roughly 10 per cent deviation) in the elastic zone of the tube when comparing with the deformable mandrel case. Also, the plastic radius is over-estimated by the model with the rigid mandrel, although the stresses in the plastic region are very close to those obtained with an elastic mandrel and the corresponding pressure inside the tube differs by only 1 per cent.

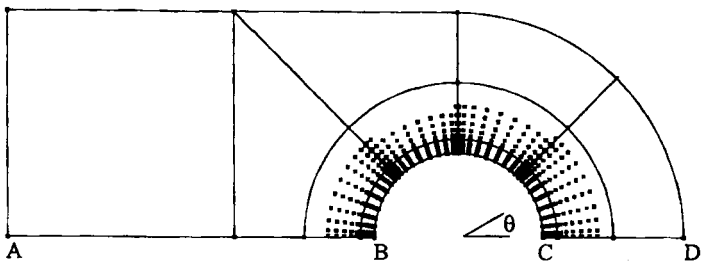

Figure 12. Mesh used in the *p*-version analysis of an attachment lug. Asterisks indicate the maximum extent of the plastic zone during cold-working

In the following, we show how to pursue a more realistic analysis.

The lug with a hole of radius $a = 1{\cdot}5$ in, outer radius $b = 4{\cdot}0$ in and total length of $l = 12$ in was modelled by 13 elements (see Figure 12). An interference level $I = 0{\cdot}02$ in was assumed between the mandrel and the lug. For the lug, we use material constants $E = 10\,000\,000$ psi, $\sigma_y = 58\,000$ psi and $\nu = 0{\cdot}3$. Symmetry conditions were used along edges A–B and C–D to reduce the computation time.

We assume that the influence of the elastic stiffness of the mandrel can be represented by a constant-stiffness distributed elastic spring interface element attached to the edge of the hole. The corresponding approximate normal spring stiffness is readily obtained from the axisymmetric linear analysis of the mandrel subject to constant pressure. The tangential stiffness of the spring is zero (no friction). Displacements corresponding to the original interference between the lug and the mandrel are now prescribed on the interface elements as an initial displacement rather than directly on the hole. Thus, we obtain a deformed shape of the hole (and the mandrel) which deviates from the circle, and a non-uniform pressure distribution reflecting the actual stiffness relation between the lug and mandrel.

The procedure suggested here for the analysis might be improved by re-calculating the spring stiffnesses, starting from the actual (non-constant) pressure distribution as applied to the mandrel, repeating the entire process with the updated data until the final check of the initial assumptions would render negligible differences. However, for the demonstration purposes of the present study, it will suffice to perform only the first step of such an iterative analysis, which is already much closer to reality than many analyses carried out in current engineering practice.

Note that the *lug* is constrained exclusively by the spring interface elements and the symmetry constraints. We consider the cold-working process in a co-ordinate system attached to the mandrel. The analysis simulates a cold-working procedure in which the *mandrel* is not capable of carrying any resultant force in the plane of the lug, but is allowed to move freely. Therefore, we obtain an equilibrated pressure distribution along the hole. The lug as a whole moves, but the left end of the model (attached to the airplane and thereby constrained) remains almost a straight line provided it is far enough from the hole.

After loading, removal of the mandrel is simulated by deleting the interface elements. At this stage, the model of the lug has only rigid body and symmetry constraints. Traction boundary conditions are given by the pressure formerly carried by the spring interface elements. We are now solving a problem which has only traction boundary conditions (except the symmetry constraint), and therefore we require the tractions to be in equilibrium.

Note that the two stages of the computation are characterized by different boundary conditions and, consequently, a different number of unknowns, and that adding or deleting elements in an existing model may change the smoothness of the exact solution. This has to be kept in mind

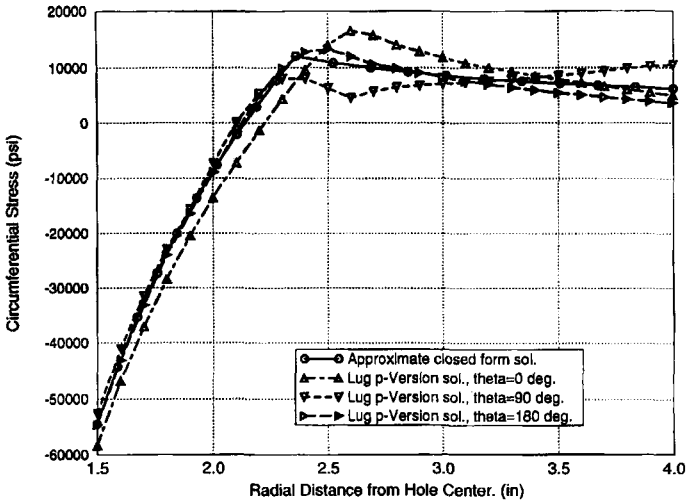

Figure 13. Cold-worked attachment lug. 'Circumferential' stresses after unloading for various locations. Comparison with analytical solution of cold-worked tube

when checking the accuracy of the corresponding purely linear solutions to ensure the use of reasonable models in the two-stage non-linear analysis.

Four interface elements were used along arc B–C. The material properties of the mandrel are the same as in all previous examples, giving a normal spring stiffness $C_n = 38\,500\,000$ psi. Figure 12 displays the maximum extent of the plastic zone during the loading as obtained by the p-version analysis with $p = 5$ (product space), corresponding to an estimated error in energy norm of less than 0·1 per cent in the elastic solutions. The maximum deviations of the internal pressure during cold-working from the constant value $P = 52\,200$ psi (corresponding to the tube) were $+8{\cdot}7$ and $-2{\cdot}5$ per cent.

In Figure 13, the 'circumferential' stress in the lug after complete unloading is compared with the solution obtained by application of the analytical solution of the *tube*. The unloading is purely elastic. Figure 13 displays the stress at $\theta = 0°$, $\theta = 90°$, and $\theta = 180°$ (cf. Figure 12). For $\theta = 0°$, the stress is much higher than the value given by the closed-form solution in the elastic zone and at the elastic-plastic interface. However, at $\theta = 90°$, the most important location for practical purposes, the analytical solution over-estimates the actual value of the stress in the elastic region closer to the hole, but under-estimates it close to the outer boundary of the lug.

This realistic problem clearly demonstrates that the simple thick-walled tube analogy reflects the actual situation of the lug only quite inaccurately whereas the p-version FEM is a very useful tool for studying elasto-plastic problems involving even complex loading and unloading conditions.

7. CONCLUSIONS

We conclude that the p-version of the finite element method performs very well in small-strain incremental elasto-plastic analysis of structures. The p-version makes it a lot easier to control the discretization error of the finite element method. Error monitoring and control is achieved automatically, with minimum user interaction, and without substantial loss of computational efficiency. In some cases, we find that the models based on the p-version yield clearly superior accuracy in comparison with their h-version counterparts.

As an example, the paper demonstrates the application of the p-version of the FEM to the cold-working problem. It is seen that the method is very well suited for this practically relevant problem and that reliable and realistic results can be obtained with a small amount of modeling work.

In summary, the application of the p-version in elasto-plastic structural analysis can be recommended.

ACKNOWLEDGEMENTS

The research work presented here has been developed while the first author was a post-doctoral research associate at the Center for Computational Mechanics, Washington University in St. Louis, MO. The second author was then working as a graduate research assistant at the same institution. The authors would like to thank Professor Barna A. Szabó for his support and interest in the work presented here, including many helpful remarks, discussions and invaluable suggestions. Furthermore, we would like to thank Mr. S. Prost-Domasky for his assistance with using the ADINA code.

The research work of the first author has been supported by the German Research Foundation DFG under grant Ho 1517/1-1. This support is gratefully acknowledged. Both authors aknowledge partial support by the Lyndon B. Johnson Space Center of the National Aeronautics and Space Administration under grant NAG 9-622. The research work of the second author has been supported in part by the Air Force Office of Scientific Research under grant F49620-93-0173.

REFERENCES

1. W. F. Chen and D. J . Han, *Plasticity for Structural Engineers*, Springer, Berlin, 1988.
2. G. Strang and G. J. Fix, *An Analysis of the Finite Element Method*, Prentice-Hall, Englewood Cliffs, N.J., 1973.
3. O. C. Zienkiewicz, *The Finite Element Method*, 3rd edn, McGraw-Hill, London, 1977.
4. C. Johnson and P. Hansbo, 'Adaptive finite element methods in computational mechanics', *Comp. Methods Appl. Mech. Eng.*, **101**, 143–181 (1992).
5. E. Stein, G. Zhang and Y. Huang, 'Modeling and computation of shakedown problems for nonlinear hardening materials', *Comp. Methods Appl. Mech. Eng.*, **103**, 247–272 (1993).
6. B. A. Szabo and I. Babuska, *Finite Element Analysis*, Wiley, New York, 1991.
7. S. M. Holzer, 'Das symmetrische Randelementverfahren: Numerische Realisierung und Kopplung mit der Finite-Elemente-Methode zur elastoplastischen Strukturanalyse', Doctoral Thesis, Technische Universität München, Berichte aus dem Konstruktiven Ingenieurbau 5/92 (ed. W. Wunderlich *et al.*), Munich, 1992.
8. B. A. Szabo, R. L. Actis and S. M. Holzer, 'Solution of elastic-plastic stress analysis problems by the p-version of the finite element method. *Modeling, Mesh Generation, and Adaptive Numerical Methods for Partial Differential Equations*', in I. Babuska, J. E. Flaherty *et al.* (eds.), IMA Volumes in Mathematics and its Applications, Vol. 75, Institute for Mathematics and its Applications, Springer, New York, 1995, pp. 395–416.
9. L. M. Katchanov, *Fundamentals of the Theory of Plasticity*, MIR, Moscow, 1974.
10. Z. Yosibash and B. A. Szabo, 'Convergence of stress maxima in finite element computations', *Comm. num. meth. eng.*, **10**, 683–697 (1994).
11. R. D. Krieg and D. B. Krieg, 'Accuracies of Numerical Solution Methods for the Elastic-perfectly Plastic Model', *ASME J. Press. Vess. Techn.*, 1977, pp. 510–515.
12. S. W. Sloan, 'Substepping schemes for the numerical integration of elastoplastic stress-strain relations', *Int. j. numer. methods eng.*, **24**, 893–911 (1987).
13. Ph.G. Hodge, 'Automatic piecewise linearization in ideal plasticity', *Comp. Methods Appl. Mech. Eng.*, **10**, 249–272 (1977).
14. M. Ortiz and J. C. Simo, 'An analysis of a new class of integration algorithms for elastoplastic constitutive relations', *Int. j. numer. methods eng.*, **23**, 353–366 (1986).
15. J. C. Naagtegal, D. M. Parks and J. R. Rice, 'On numerically accurate finite element solutions in the fully plastic range', *Comp. Methods Appl. Mech. Eng.*, **4**, 153–177 (1974).
16. I. Babuska and M. Suri, 'On locking in the finite element method', *SIAM J. Numer. Anal.*, **29**(5), 1261–1293 (1992).
17. I. Babuska and M. Suri, 'Locking effects in the finite element approximation of elasticity problems', *Numer. Math.*, **62**, 439–439 (1992).

18. M. Vogelius, 'An analysis of the *p*-version of the finite element method for nearly incompressible materials. Uniformly valid optimal error estimates', *Numer. Math.*, **41**, 39–53 (1983).
19. W. Prager and Ph. G. Hodge, *Theory of Perfectly Plastics Solids*, Wiley, New York, 1951.
20. D. L. Rich, L. F. Impellizzeri, Fatigue analysis of cold-worked and interference-fit fastener holes, in *Cyclic Stress-strain and Plastic Deformation Aspects of Fatigue Crack Growth*, American Society of Testing Materials, Special Technical Publication 637, 1977.
21. ADINA User's Manual, ADINA R&D, Inc. Watertown, Massachusetts, 1992.
22. Th. Sussmann and K.-J. Bathe, 'A finite element formulation for nonlinear incompressible elastic and inelastic analysis', *Comput. Struct.*, **26**, 357–409 (1987).